

# A Target-Mediated Drug Disposition Model to Explain Nonlinear Pharmacokinetics of the $11\beta$ -Hydroxysteroid Dehydrogenase Type I Inhibitor SPI-62 in Healthy Adults

The Journal of Clinical Pharmacology  
2021, 61(11) 1442–1453  
© 2021 Sparrow Pharmaceuticals, Inc.  
The *Journal of Clinical Pharmacology*  
published by Wiley Periodicals LLC on  
behalf of American College of Clinical  
Pharmacology  
DOI: 10.1002/jcph.1925

Nan Wu, MS<sup>1</sup>, David A. Katz, PhD<sup>2</sup> , and Guohua An, MD, PhD<sup>1</sup> 

## Abstract

SPI-62 is a selective and potent small-molecule inhibitor of  $11\beta$ -hydroxysteroid dehydrogenase type I (HSD-1). SPI-62 has demonstrated substantial and complex nonlinear pharmacokinetics (PK) in humans that is characterized by unusually low plasma exposure at low doses, dose-dependent volume of distribution, nonlinear PK following the first dose, and dose-proportional PK at steady state, as well as unusually high accumulation ratios at low doses. The most likely explanation for the observed nonlinearity of SPI-62 is the saturable binding of SPI-62 to its pharmacological target HSD-1, a phenomenon known as target-mediated drug disposition (TMDD). Because of the nonlinear and complex PK of SPI-62, the relationship among SPI-62 dose, exposure, and response is no longer intuitive and consequently dose selection can be challenging. To facilitate dose selection and clinical trial design, in the current study population PK analysis was performed to characterize SPI-62 dose-exposure relationship in humans quantitatively. SPI-62 PK was best characterized by a 2-compartment TMDD model with 3 transit absorption compartments. The model was successfully established to explain the substantial and unusual nonlinear PK of SPI-62 in humans, and it provided adequate fitting for both single- and multiple-dose data. Our modeling work has provided a strong foundation for dose selection in future SPI-62 clinical trials.

## Keywords

target-mediated drug disposition,  $11\beta$ -hydroxysteroid dehydrogenase type I inhibitor, nonlinear pharmacokinetics, drug development, population PK modeling

$11\beta$ -hydroxysteroid dehydrogenase type I (HSD-1) converts inactive cortisone to active cortisol in tissues, including liver, fat, brain, bone and eye,<sup>1</sup> in which cortisol regulates a range of physiological functions, including glucose and lipid metabolism, mood, memory, sleep, osteoblast turnover, and intraocular pressure.<sup>2</sup> Cushing's syndrome and autonomous cortisol secretion (ACS) are conditions of cortisol excess that are associated with considerable metabolic, cardiovascular, bone, and other morbidities as well as a substantial mortality risk.<sup>3,4</sup> HSD-1 acts similarly on the corticosteroid medicines, for example, it converts inactive prednisone to active prednisolone.<sup>5</sup> The corticosteroids are associated with  $\approx 10\%$  of all drug adverse events including those that result in hospitalization.<sup>6</sup> The role of HSD-1 in the biology of cortisol and the corticosteroid medicines suggests that HSD-1 inhibitors would have strong potential to benefit patients with Cushing's syndrome or ACS or who rely on long-term use of corticosteroid medicines to control autoimmune diseases and other conditions. Supportive evidence includes that patients with both severe hypercortisolism because of a Cushing's tumor and low constitutional HSD-1 activity showed no cortisol-related symptoms.<sup>7,8</sup> Furthermore, HSD-1-knockout mice resist multiple adverse effects

of administered corticosteroids, and HSD-1 inhibitors have blocked certain corticosteroid adverse effects in animal models.<sup>9–11</sup>

SPI-62 (formerly known as ASP3662) is a novel, potent, and selective small-molecule HSD-1 inhibitor with high affinity against human HSD-1 ( $K_i$ , 5.3 nM, measured in vitro using purified enzyme).<sup>12</sup> SPI-62 is in development as a treatment for Cushing's syndrome and ACS and as adjunctive therapy to prednisolone in patients with polymyalgia rheumatica.

<sup>1</sup>Division of Pharmaceutics and Translational Therapeutics, College of Pharmacy, University of Iowa, Iowa City, Iowa, USA

<sup>2</sup>Sparrow Pharmaceuticals, Inc., Portland, Oregon, USA

This is an open access article under the terms of the Creative Commons Attribution-NonCommercial-NoDerivs License, which permits use and distribution in any medium, provided the original work is properly cited, the use is non-commercial and no modifications or adaptations are made.

Submitted for publication 22 December 2020; accepted 8 June 2021.

## Corresponding Author:

Guohua An, MD, PhD, Division of Pharmaceutics and Translational Therapeutics, College of Pharmacy, University of Iowa, 115 S. Grand Ave., Iowa City, IA 52242, USA  
Email: guohua-an@uiowa.edu

**Table 1.** Summary of SPI-62 Clinical PK Data Included During TMDD Model Development

Study	Sample Size	Dose Regimen	Sampling Times	LLOQ (ng/mL)
SAD/FE trial <sup>a</sup>	6	1 mg, single dose	0.5, 1, 1.5, 2, 3, 4, 6, 8, 10, 12, 18, 24, 36, 48, and 72 hours postdose for 1-, 3-, and 10-mg cohorts; additional 96 and 120 hours postdose for 6 mg cohort	0.1
	6	3 mg, single dose		
	6	6 mg, single dose		
	6	10 mg, single dose		
MAD study <sup>a</sup>	4	3 mg loading dose on day 1, 0.2 mg once-daily dose on days 2-14	0.5, 1, 1.5, 2, 3, 4, 8, 12, 16, and 24 hours after the first dose; 0.5, 1, 1.5, 2, 3, 4, 8, 12, 16, 24, 48, 72, 96, 120, 144, and 168 hours after the last dose for 0.2- and 0.4-mg cohorts	0.004
	4	0.4 mg once-daily doses on days 1-14		
	6	0.7 mg single dose on day 1, 0.7-mg once-daily doses on days 7-20		
	6	2 mg single dose on day 1, 2 mg once-daily doses on days 7-20		

SAD, single ascending dose; MAD, multiple ascending dose; LLOQ, lower limit of quantification.

<sup>a</sup> More doses were evaluated in the original clinical trials. Data from higher-dose groups were not used in the model development and therefore are not presented in this table.

The safety, pharmacokinetics (PK), and pharmacodynamics (PD) of SPI-62 in healthy adults were previously evaluated in 2 phase 1 clinical trials: a first-in-human (FIH) single-ascending-dose (SAD) and food-effect (FE) trial and a multiple-ascending-dose (MAD) trial.<sup>12</sup> The results showed that SPI-62 has substantial and complex nonlinear PK in humans that is characterized by unusually low plasma exposure at low doses, dose-dependent volume of distribution, nonlinear PK following the first dose and dose-proportional PK at steady state, and unusually high accumulation ratios at low doses, which cannot be explained by the drug's known elimination half-life. This nonlinear PK appeared to be caused by the saturable binding of SPI-62 to its pharmacological target, HSD-1, a phenomenon known as target-mediated drug disposition (TMDD).<sup>13,14</sup> Because of the nonlinear and complex PK of SPI-62, the relationship among SPI-62 dose, exposure, and response is no longer intuitive and consequently dose selection can be challenging. To address this need, in the current study population PK analysis was performed to characterize SPI-62 dose-exposure relationship in healthy adults quantitatively following single and multiple doses.

## Methods

### Data Source

Two phase 1 clinical trials, a SAD/FE trial and a MAD trial, have been conducted to evaluate the safety and PK of SPI-62 in healthy adults.<sup>12</sup> In both the SAD/FE and MAD trials, SPI-62 exhibited substantial nonlinear PK after single low doses and demonstrated essentially linear PK at doses > 10 mg. Accordingly, SPI-62 PK data from high-dose groups (> 10 mg) were considered not informative for dose selection for future

clinical trials. Therefore, only the data from ≤10-mg dose groups were included in the current population PK analysis. The dose regimen and sampling schedule of the data used in our analysis are summarized in Table 1 and briefly described below.

**Data used from SAD/FE trial.** This trial was an FIH randomized, double-blind, placebo-controlled, parallel-group escalating-dose study. A total of 48 subjects were enrolled in 6 dose cohorts (1, 3, 6, 10, 30, and 60 mg). Eight subjects were included in each cohort, among which 6 subjects received a single dose of SPI-62 and 2 subjects received placebo. SPI-62 or placebo was given under fasted conditions. The data included in our analysis were from doses up to 10 mg (Table 1). In the 1-, 3-, and 10-mg cohorts, venous blood samples were collected 0.5, 1, 1.5, 2, 3, 4, 6, 8, 10, 12, 18, 24, 36, 48, and 72 hours after dose administration. In the 6-mg cohort, venous blood samples were collected 0.5, 1, 1.5, 2, 3, 4, 6, 8, 10, 12, 18, 24, 36, 48, 72, 96, and 120 hours after dose administration.

**Data used from MAD trial.** This trial included 2 separate parts: part A for high-dose (10-50 mg SPI-62 once daily) cohorts and part B for low-dose cohorts. Data from part A were not included in our analysis, and therefore are not described here. part B was an open-label, nonrandomized trial to characterize the PK and PD effect of SPI-62 at lower doses (0.2, 0.4, 0.7, and 2 mg) in healthy subjects. In the 0.2-mg cohort, 4 subjects received a loading dose of 3 mg SPI-62 on day 1 followed by once-daily doses of 0.2 mg on days 2-14. In the 0.4-mg cohort, 4 subjects received SPI-62 0.4 mg once daily for 14 days (days 1-14). PK samples in these 2 cohorts were collected 0.5, 1, 1.5, 2, 3, 4, 8, 12, 16,

and 24 hours after the first dose; 0.5, 1, 1.5, 2, 3, 4, 8, 12, 16, 24, 48, 72, 96, 120, 144, and 168 hours after the last dose.

The cohorts of 0.7 and 2 mg were designed to collect PK data after both single and multiple dosing of SPI-62 0.7 or 2 mg. Subjects ( $n = 6$  for each cohort) received a single dose of SPI-62 on day 1, followed by a 6-day washout period and once-daily doses of SPI-62 for 14 days (days 7-20). PK samples in these 2 cohorts were collected 0.5, 1, 1.5, 2, 3, 4, 8, 12, 16, 24, 36, 48, 72, 96, 120, and 144 hours after the first dose and 0.5, 1, 1.5, 2, 3, 4, 8, 12, 16, 24, 48, 72, 96, 120, 144, and 168 hours after the last dose.

Plasma concentrations of SPI-62 were determined using a validated liquid chromatography-tandem mass spectrometry assay.<sup>12</sup> Both assay validation and clinical sample analysis were performed in a good laboratory practice environment. The lower limit of quantification (LLOQ) for SPI-62 was 0.1 ng/mL in the SAD study and 0.004 ng/mL for samples from part B of the MAD study. A total of 996 plasma concentrations, including 774 above the LLOQ and 222 below the LLOQ, were used in the population modeling analysis. These data were from 44 subjects, including 33 male and 11 female subjects, with an average bodyweight of  $76.5 \pm 12.1$  kg and age ranging from 20 to 54 years.

#### Population Pharmacokinetics Modeling

All SPI-62 PK data were analyzed simultaneously using the nonlinear mixed-effects modeling approach with NONMEM (version 7.4.3; Icon Development Solutions, Ellicott City, Maryland) interfaced with Pirana (version 2.9.9; <http://www.pirana-software.com/>). The first-order conditional estimation method with interaction and a user-defined subroutine (ADVAN13) were used to estimate the population mean values of the PK parameters, interindividual variability (IIV), and residual variability (RV). RStudio 4.0.2 (RStudio, PBC, Boston, Massachusetts) and Sigmaplot 13.0 (Systat Software, San Jose, California) were used for data handling and graphical analysis.

**Structural model.** As the substantial nonlinear PK behaviors of SPI-62 in humans were fully in line with the known TMDD principles for small-molecule compounds,<sup>15,16</sup> models with TMDD components were tested directly. Several TMDD models were explored during the model-building process, including different compartment models (eg, 1-compartment vs 2-compartment) as well as different number of transit compartments (0, 1, 2, 3, and 4 transits) during the absorption process. Among all models tested, the best model was found to be a 2-compartment TMDD model with 3 transit compartments between the absorption site (ie, depot compartment) and the central compart-

ment (Figure 1). In this model, the absorption process of SPI-62 was characterized by 4 sequential first-order transition rate constants ( $K_{tr}$ ). After SPI-62 reaches the central compartment ( $C_{\text{central}}$ ,  $V_{\text{central}}$ ), the drug molecules can distribute to the peripheral compartment ( $C_{\text{peripheral}}$ ,  $V_{\text{peripheral}}$ ) by distribution flow ( $Q$ ), be eliminated from the system by a linear elimination pathway that is characterized by  $CL/V$ , or bind to a target ( $R$ ) with a second-order association rate constant ( $k_{\text{on}}$ ) to form an SPI-62:R complex. The interaction between SPI-62 and the target is a reversible process. After the SPI-62:R complex is formed, it will eventually dissociate back to free drug and free target with a first-order dissociation rate constant ( $k_{\text{off}}$ ). In contrast to large-molecule compounds, in general, small-molecule drug:R complexes do not undergo lysosomal degradation.<sup>14</sup> Therefore, in the SPI-62 model structure, there is no  $k_{\text{int}}$  (ie,  $k_{\text{int}} = 0$ ). The total number of binding sites ( $R_{\text{total}}$ ) was assumed to be constant. Accordingly, there is no need to write a differential equation for free target ( $R$ ), which is instead represented as ( $R_{\text{total}} - RC$ ).

The following equations were used to characterize the model:

The equations for the absorption compartment (with 3 transit components) were:

$$\frac{dA_{\text{depot, SPI62}}}{dt} = -k_{tr} \times \text{Dose} \quad (1)$$

$$A_{\text{depot, SPI62}}(0) = \text{Dose}$$

$$\frac{dA_{\text{Trans1, SPI62}}}{dt} = k_{tr} \times A_{\text{depot, SPI62}} - k_{tr} \times A_{\text{Trans1, SPI62}} \quad (2)$$

$$A_{\text{Trans1, SPI62}}(0) = 0$$

$$\frac{dA_{\text{Trans2, SPI62}}}{dt} = k_{tr} \times A_{\text{Trans1, SPI62}} - k_{tr} \times A_{\text{Trans2, SPI62}} \quad (3)$$

$$A_{\text{Trans2, SPI62}}(0) = 0$$

$$\frac{dA_{\text{Trans3, SPI62}}}{dt} = k_{tr} \times A_{\text{Trans2, SPI62}} - k_{tr} \times A_{\text{Trans3, SPI62}} \quad (4)$$

$$A_{\text{Trans3, SPI62}}(0) = 0$$

The equation for the central compartment was:

$$\begin{aligned} \frac{dA_{\text{central, SPI62}}}{dt} = & k_{tr} \times A_{\text{Trans3, SPI62}} - k_{\text{on}} \\ & \times C_{\text{central, SPI62}} \times (R_{\text{total}} - RC) + k_{\text{off}} \\ & \times RC - CL/V_{\text{central, SPI62}} \times A_{\text{central, SPI62}} \\ & - Q/V_{\text{central, SPI62}} \times A_{\text{central, SPI62}} \\ & + Q/V_{\text{peripheral, SPI62}} \times A_{\text{peripheral, SPI62}} \end{aligned} \quad (5)$$

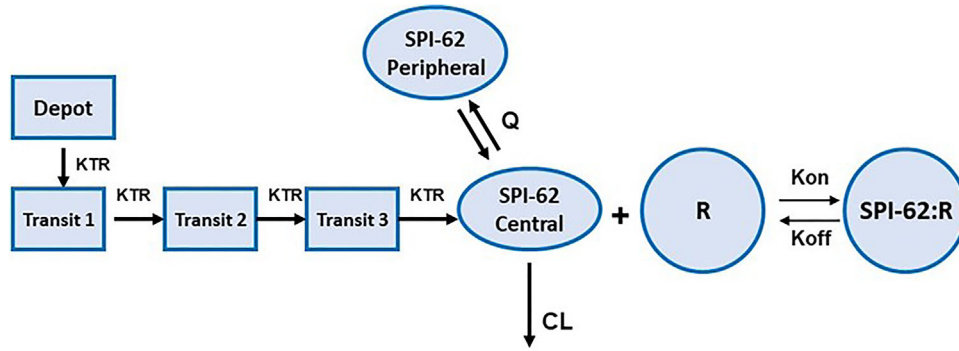


**Figure 1.** Final model structure used to characterize the pharmacokinetics of SPI-62 in humans. SPI-62 was absorbed from the depot following 3 transit compartments with first-order absorption rate constant ( $k_{tr}$ ) and eliminated from the central compartment characterized by  $CL/V$ . SPI-62 in the central compartment can distribute to the peripheral compartment by distribution flow ( $Q$ ) or bind with HSD-1 (ie,  $R$ ) with second-order association rate constant ( $k_{on}$ ) to form SPI-62:R complexes. SPI-62:R can dissociate back to free drug and free HSD-1 target with the first-order dissociation rate constants ( $k_{off}$ ). The total amount of HSD-1 in humans ( $R_{total}$ ) is assumed to be constant.

$$A_{central, SPI62} (0) = 0$$

The equation for the peripheral compartment was:

$$\frac{dA_{peripheral, SPI62}}{dt} = Q/V_{central, SPI62} \times A_{central, SPI62} - Q/V_{peripheral, SPI62} \times A_{peripheral, SPI62} \quad (6)$$

$$A_{peripheral, SPI62} (0) = 0$$

The equation for the binding with the high-affinity/low-capacity site compartment was:

$$\frac{dRC}{dt} = k_{on} \times C_{central, SPI62} \times (R_{total} - RC) - k_{off} \times RC \quad (7)$$

$$RC (0) = 0$$

where  $RC$  represents the amount of the SPI-62:R complex and  $R_{total}$  represents the total amount of binding sites.

**Stochastic model.**

- *Interindividual variability (IIV):* All IIV of the PK parameters of SPI-62 was estimated by an exponential model as follows:

$$P_i = TVP \cdot \exp(\eta_i) \quad (8)$$

where  $\eta_i$  is the proportional difference between the parameter estimate of the  $i$ th subject ( $P_i$ ) and the typical population parameter (ie, mean estimate) value ( $TVP$ ),  $\eta_i$  is assumed to be normally distributed with a mean of 0 and a variance of  $\omega^2$ .

- *Residual variability (RV):* Additive, proportional, and a combined proportional and additive RV models were evaluated. Following is an example of the

proportional error model evaluated for SPI-62 PK,

$$C_{ij} = \bar{C}_{ij} (1 + \varepsilon_{ij}) \quad (9)$$

where  $C_{ij}$  is the measured plasma concentration of SPI-62 for the  $i$ th individual at time  $j$ ,  $\bar{C}_{ij}$  is the corresponding model predicted concentration in the same subject at the same time, and  $\varepsilon_{ij}$  is the proportional error, which is assumed to be normally distributed with a mean of 0 and a variance of  $\sigma^2$ .

**Covariate model.** The covariates evaluated in the analysis included age, sex, body weight, and race. Prior to covariate model tests, exploratory analyses were performed. The random effects of the PK parameters obtained from the model fitting were plotted against these 4 covariates. During the covariate test, forward addition was applied first to determine significant covariates. Only covariates that decreased the objective function value by more than 3.84 (corresponding to  $P < .05$ ) compared with the base model were considered for the full covariate selection. Backward elimination was then applied to remove covariates from the model with an increase in the objective function value  $> 6.63$  (corresponding to 1  $df$  at  $P < .01$ ). Only covariates that produced this magnitude of increase were retained in the model.

**Model evaluation.** The final model was selected based on the stability of parameter estimates and objective function values, biological and physiological plausibility of parameter estimates, and goodness-of-fit plots. The likelihood ratio test was used for comparing nested models in which a decrease in the NONMEM objective function ( $-2 \log$  likelihood) of 3.84 points was necessary to consider the improvement in model performance statistically significant at  $\alpha = 0.05$ .

A prediction-corrected visual predictive check (pcVPC) was performed to evaluate the predictive ability of the final model. Using the original data set, the final model and its parameter estimates, 1000 virtual observations at each sampling point were simulated. The observed concentrations (prediction corrected) as well as the median and 5th and 95th percentiles of the observed data were plotted with the 95% confidence intervals of the simulated median and 5th and 95th percentiles. If the model is consistent and appropriate, the 5th, 50th, and 95th percentiles of the observed data should fall within the 95% confidence intervals of the 5th, 50th, and 95th percentiles of the simulated concentrations. The condition number (ratio of the largest and the smallest eigenvalues) was calculated, and the model is considered overparametrized or ill-conditioned if the calculated value is  $>1000$ .

## Results

### Clinical PK Data

A useful way to evaluate if a drug has linear pharmacokinetics is to plot dose-normalized concentration-time profiles. Drugs with linear pharmacokinetics have overlapped concentration/dose-versus-time profiles, whereas the profiles from drugs with nonlinear pharmacokinetics do not superimpose as their kinetics do not obey the rule of superposition. Figure 2 shows dose-normalized SPI-62 plasma concentration-time profiles following single oral doses in the SAD/FE trial (Figure 2A) or multiple oral once-daily doses in the MAD trial on day 1 (Figure 2B) or the last day (Figure 2C). As shown in Figure 2A, following single doses, the dose-normalized pharmacokinetic profiles tended to superimpose in those high-dose groups ( $\geq 6$  mg) but not in low-dose groups, with a greater extent of deviation as dose was lower. This indicated that nonlinear pharmacokinetics of SPI-62 occurred at low doses, with more substantial nonlinearity at lowest doses. Similarly, dose-normalized day 1 data from the MAD trial also showed non-overlapping profiles (Figure 2B), further confirming that SPI-62 has substantial nonlinear PK at low doses when it was given for the first time. Interestingly, the nonlinear pharmacokinetics observed after the first dose disappeared after repeated doses, as reflected by the superimposed PK profiles across all dose groups on the last day of dosing in the MAD trial (Figure 2C).

### Population PK Modeling

**Goodness of model fitting.** As shown in Figure 1, the final model was a 2-compartment model that incorporated 3 transit absorption compartments with binding to a high-affinity, low-capacity target site. The time course of mean observed versus population-

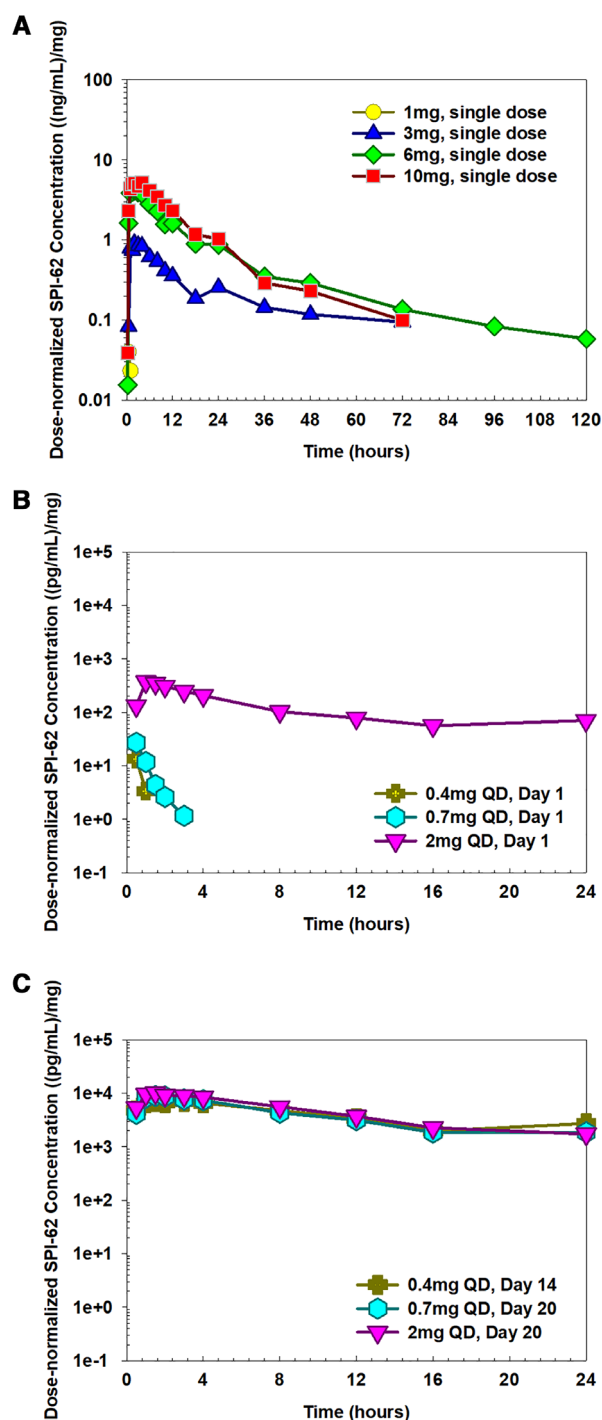


**Figure 2.** Dose-normalized mean plasma concentration-time course of SPI-62 following (A) single oral doses of SPI-62, (B) multiple once-daily doses on day 1 after the first dose of SPI-62, and (C) multiple once-daily doses after the last dose of SPI-62.

predicted plasma concentrations of SPI-62 following single or multiple ascending doses in humans are presented in Figures 3 and 4, respectively. As shown in these 2 figures, the proposed TMDD model adequately captured SPI-62 plasma concentration-time profiles in both the SAD and MAD trials, as reflected

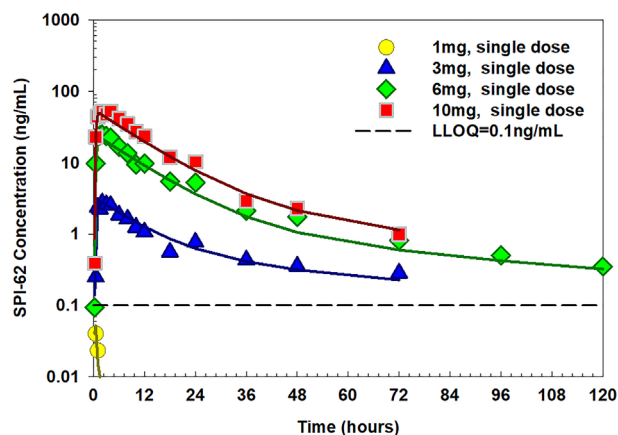


**Figure 3.** Time courses of observed (symbols) and model-predicted (lines) SPI-62 plasma concentrations following 1-, 3-, 6-, 10-mg single oral doses of SPI-62 in healthy adults.

by the close agreement between the model-predicted SPI-62 concentrations and observed concentrations at various points across different doses. In addition to the observed and population-predicted SPI-62 plasma concentration-time profiles, other standard goodness-of-fit plots have also been evaluated. As shown in Figure 5, the individual-predicted and population-predicted concentrations versus the observed SPI-62 concentrations were evenly distributed around the line of identity without bias (Figure 5A,B), indicating that the final TMDD model characterized SPI-62 adequately at both the individual and population levels. In addition, the conditional weighted residuals appear distributed uniformly around the zero line when plotted by either time or population-predicted concentrations (Figure 5C,D), further confirming that there was no significant bias in the model fit.

To evaluate the predictive ability of the final model, pcVPC was performed. As shown in Figure 6, most

of the observed concentrations were within the 95% prediction intervals from the simulation data, indicating that the prediction-corrected concentrations were well predicted by the final model. The somewhat larger magnitude of model-predicted compared with observed variability had no influence on confidence in the simulation results.

**Parameter estimation.** Age, body weight, race, and sex were tested as covariates on SPI-62 PK parameters, and none of them showed any significant impact. The final estimates of the SPI-62 PK parameters from the final TMDD model are presented in Table 2. The apparent clearance of SPI-62 was estimated to be 10.1 L/h, indicating that it is a low extraction ratio compound. The apparent volume of distribution in the central and peripheral compartments was estimated to be 141 and 114 L, respectively. Model results indicated that SPI-62 interacted with its target with fast association and slow dissociation processes, as reflected by a high  $k_{on}$  value ( $7.10 \text{ nM}^{-1}\text{h}^{-1}$ ) and a much smaller  $k_{off}$  value ( $0.249 \text{ h}^{-1}$ ). The total amount of the target was estimated to be 6070 nmol.

In the final model, IIV terms were placed on the volume of distribution in the central compartment, clearance, and transit absorption rate constant, dissociation rate constant, and the total amount of the target; a proportional error model was found to best describe the unexplained residual variability. As shown in Table 2, the relative standard error (%RSE) was below 30% for all estimated PK parameters and within  $\approx 50\%$  for most IIV and RV terms. The calculated shrinkage values for etas in the final model were all below 30%, indicating that diagnostic plots shown earlier were informative and reliable for model evaluation. Condition number (calculated from the ratio of the largest and the smallest eigenvalues) of the final model was 24.6, which is much

**Table 2.** Estimated Parameters From the Final TMDD Model for SPI-62

Parameter	Unit	Definition	Estimate	RSE (%)	Shrinkage (%)
$V_{\text{central}}^a$	L	Volume of distribution at central compartment	141	16	
CL <sup>a</sup>	L/h	Clearance	10.1	6	
$Q^a$	L/h	Distribution flow	2.31	12	
$V_{\text{peripheral}}^a$	L	Volume of distribution at peripheral compartment	114	7	
$K_{tr}$	$\text{h}^{-1}$	Transit absorption rate constant	8.52	11	
$K_{on}$	$\text{nM}^{-1}\text{h}^{-1}$	Association rate constant	7.1	7	
$K_{off}$	$\text{h}^{-1}$	Dissociation rate constant	0.249	24	
$R_{\text{total}}$	nmol	Total receptor amount	6070	9	
IIV <sub><math>V_{\text{central}}</math></sub>	%	Interindividual variability on $V_{\text{central}}$	54.3%	27	14
IIV <sub>CL</sub>	%	Interindividual variability on CL	20.6%	59	22
IIV <sub><math>K_{tr}</math></sub>	%	Interindividual variability on $K_{tr}$	50.6%	29	8
IIV <sub><math>K_{off}</math></sub>	%	Interindividual variability on $K_{off}$	116%	50	15
IIV <sub><math>R_{\text{total}}</math></sub>	%	Interindividual variability on $R_{\text{total}}$	35.8%	38	12
$\sigma^2$	%	Proportional residual variability	26.8%	2	7

<sup>a</sup>Please note these are apparent parameters as bioavailability (F) is unknown.

### 3mg Loading Dose

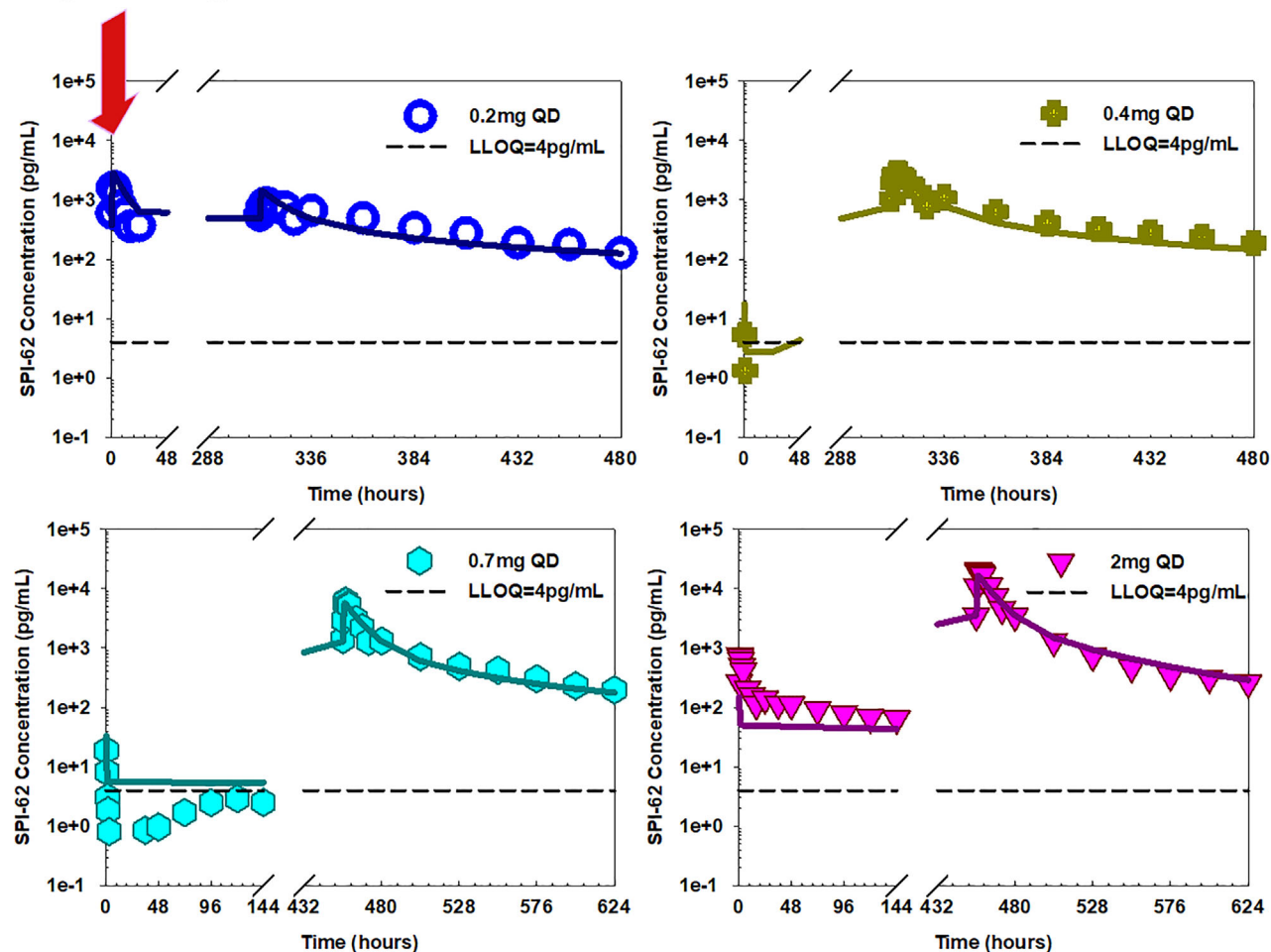


**Figure 4.** Time courses of observed (symbols) and model-predicted (lines) SPI-62 plasma concentrations following 0.2-, 0.4-, 0.7-, and 2-mg oral multiple doses of SPI-62 in healthy adults.

lower than the cutoff of 1000; this indicates that the final TMDD model was not overparametrized or ill-conditioned.

To further evaluate the model performance, the model-estimated parameters of SPI-62, including  $AUC_{inf}$ ,  $C_{max}$ , and  $t_{1/2}$  following single doses and  $AUC_t$  and  $C_{max}$  on day 1 and the last day following multiple doses were compared with those obtained from noncompartmental analysis (NCA) using the observed data<sup>12</sup> (Table 3, Figure 7, and Appendix 1). As shown in the upper panel of Table 3, model-predicted values and NCA estimated values were in close agreement in 6- and 10-mg single-dose groups. The observed exposures, especially  $AUC_{inf}$ , in 1- and 3-mg single-dose groups were unusually low and were not calculated in NCA; our model accurately captured this phenomenon, as reflected by the very low values of the predicted SPI-62 exposures. Similarly, model-predicted values were in good agreement with NCA estimated values in all

multiple-dose groups (Table 3, lower panel). Our model adequately captured the extremely low exposures of SPI-62 following the first low doses (ie,  $AUC_{24,first-dose}$  and  $C_{max,first-dose}$ ) and dose proportional increases in exposure after repeated doses (ie,  $AUC_{24,last-dose}$  and  $C_{max,last-dose}$ ). In addition, the accumulation of SPI-62 after repeated doses was evaluated. Accumulation ratios were calculated using  $C_{max}$  ratios instead of AUC ratios because AUC is sensitive to the level of censoring and consequently may not provide reliable estimation. Our model predicted that the accumulation ratios in 0.4-, 0.7-, and 2-mg groups were 117.4, 170.0, and 110.6, respectively; these values were in line with the accumulation ratios calculated using observed  $C_{max}$  values.

### Discussion

SPI-62 demonstrated substantial and unusual nonlinear PK when its disposition was evaluated over a wide

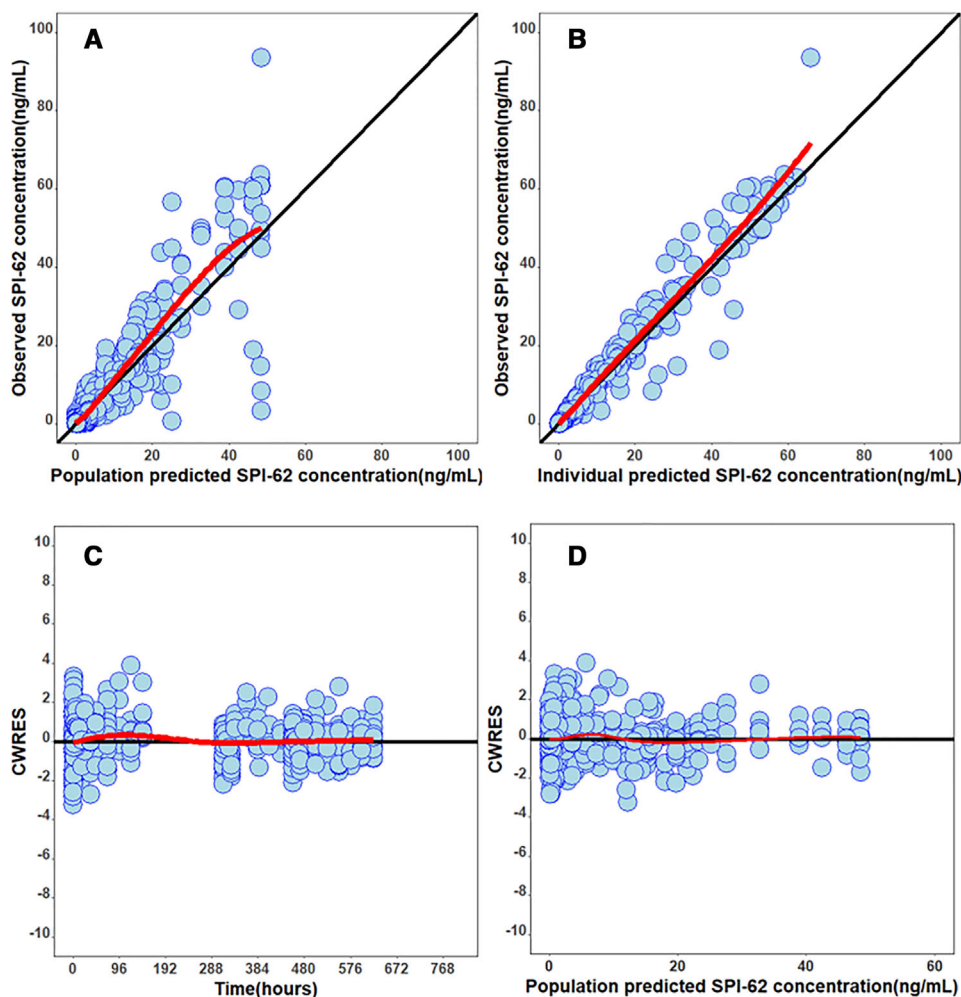


**Figure 5.** Goodness-of-fit plots for the final model of SPI-62. (A) Observed versus population-predicted SPI-62 plasma concentrations, (B) observed versus individual-predicted SPI-62 plasma concentrations, (C) weighted residuals versus time, (D) weighted residuals versus population-predicted SPI-62 plasma concentrations. Solid black lines represent lines of identity in (A) and (B) and zero residuals in (C) and (D). Trend lines are shown in red.

dose range in FIH SAD/FE and MAD clinical trials. Based on its overall nature of kinetics, the most likely explanation for the observed nonlinearity of SPI-62 is the specific binding of SPI-62 to a high-affinity, low-capacity target site. Because of the low-capacity feature of the target, nonlinear pharmacokinetics mediated by the target mainly occurred at low doses. Following low doses, because of its high affinity, the target rapidly acquired a large fraction of the administered SPI-62 dose so that only a small portion of the administered drug was available in systemic circulation. As a result, the SPI-62 plasma concentrations were unusually low, as most drug molecules were trapped by its target located in tissues. With increase in SPI-62 doses, the low-capacity target was saturated, and SPI-62 demonstrated linear pharmacokinetics at high doses because the portion sequestered by the target was small relative to the total dose. When the same subject received repeated doses, the drug molecules from previous doses

were still bound to the target because of the high affinity of the target site. As a result, the portion of the later doses that was trapped by the target was smaller and smaller. As the target has low capacity, it was saturated with repeated low doses, and consequently SPI-62 demonstrated linear pharmacokinetics at steady state.

In the current study, for the first time we report the model-based population PK analysis of SPI-62 in healthy adults. The substantial nonlinear PK of SPI-62 was best characterized by a 2-compartment TMDD model with 3 transit absorption compartments. The concept of TMDD was coined by Levy in 1994 to describe a special source of nonlinearity caused by saturable binding of the drug to a high-affinity, low-capacity pharmacological target such as an enzyme or a receptor.<sup>13</sup> Both large-molecule and small-molecule compounds can have TMDD, but they demonstrate substantially different nonlinear

**Table 3.** Comparison of Model-Predicted Versus Observed Pharmacokinetics Parameters of SPI-62 in Healthy Adults Following Single Ascending Doses (Upper) or Multiple Ascending Doses (Lower)

		SAD/FE Trial							
		1 mg (n = 6)		3 mg (n = 6)		6 mg (n = 6)		10 mg (n = 6)	
Pharmacokinetics Parameters	Unit	Observed	Predicted	Observed	Predicted	Observed	Predicted	Observed	Predicted
AUC <sub>inf</sub>	ng·hour/mL	NC	57.28	52.58 (82.9%)	64.45	366.7 (45.9%)	362.3	759.0(25.6%)	714.8
C <sub>max</sub>	ng/mL	0.1296 (155.6%)	0.05193	1.903 (109.9%)	2.879	25.65 (40.1%)	22.42	62.63 (24.1%)	48.52
t <sub>1/2</sub>	hour	NC	4218	50.72 (32.7%)	42.99	39.73 (28.5%)	54.20	18.71 (32.9%)	21.95
		MAD Trial							
		0.4 mg (n = 4)		0.7 mg (n = 6)		2 mg (n = 6)			
		Observed	Predicted	Observed	Predicted	Observed	Predicted		
AUC <sub>24,first dose</sub>	ng·h /mL	NC	0.07316	NC	0.1472	NC	1.246		
AUC <sub>24,last dose</sub>	ng·h/mL	36.94 (7.0%)	39.12	62.33 (24.9%)	69.42	213.6 (11.6%)	198.9		
C <sub>max,first dose</sub>	ng/mL	0.00942,0.01207*	0.01755	0.01850 (132.1%)	0.03330	0.4106 (124.6%)	0.1485		
C <sub>max,last dose</sub>	ng/mL	2.949 (8.3%)	3.113	6.499 (28.5%)	5.662	20.71 (24.47%)	16.42		
AR <sub>Cmax</sub>		NC	177.4	369.8 (49.4%)	170.0	66.33 (72.7%)	110.6		

NC, not calculated; AUC<sub>inf</sub>, area under the concentration-time curve from time 0 to infinity; C<sub>max</sub>, maximum concentration; AUC<sub>0-24h</sub>, area under the concentration-time curve from 0 extrapolated to 24 hours; t<sub>1/2</sub>, terminal elimination half-life; AUC<sub>24,first dose</sub>, area under plasma concentration-time curve over 24-hour interval on day 1; AUC<sub>24,last dose</sub>, area under the steady-state plasma concentration-time curve to the dosing interval; C<sub>max,first dose</sub>, maximum plasma concentration over 24-hour interval on day 1; C<sub>max,last dose</sub>, steady-state maximum plasma concentration; AR<sub>Cmax</sub>, accumulation ratio calculated based on C<sub>max,last dose</sub> over C<sub>max,first dose</sub>.

All observed data are presented as geometric mean (CV%). CV% is not presented for predicted data, as they were obtained using population predicted SPI-62 concentrations.

\*On day 1, only 2 subjects had plasma concentration levels > LLOQ; individual values are presented.

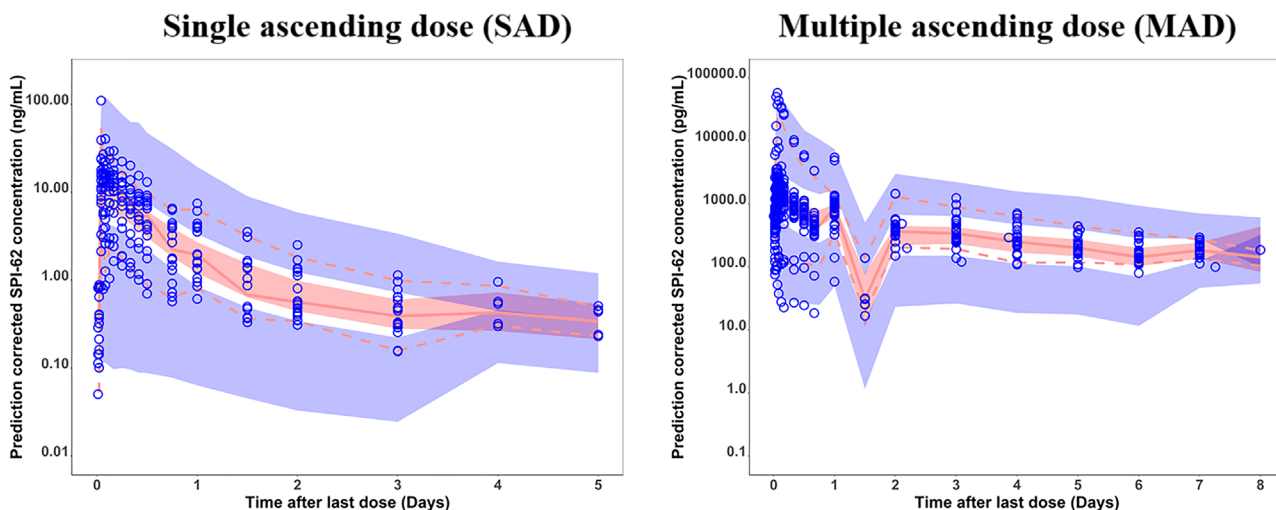
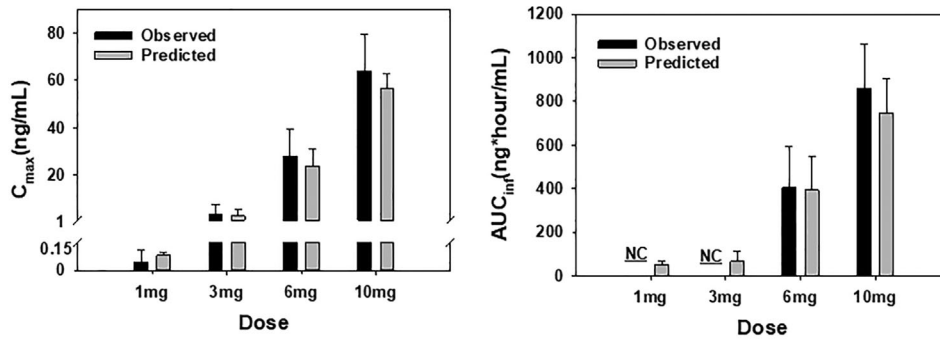


**Figure 6.** Prediction-corrected visual predicted check (pcVPC) of plasma SPI-62 data. The observed plasma concentrations (prediction corrected) are represented by blue circles. The solid red line represents the median prediction-corrected plasma concentration, and the semitransparent red field represents a simulation-based 95% confidence interval for the median. The observed 5% and 95% percentiles are presented with dashed red lines, and the 95% confidence intervals for the corresponding model-predicted percentiles are shown as semitransparent blue fields.

pharmacokinetic behaviors because the former is mainly driven by target-mediated elimination, whereas the latter is mainly affected by target-mediated distribution.<sup>14</sup> For small-molecule compounds exhibiting TMDD with target located in tissues, the

key features include (1) nonlinear pharmacokinetics at low doses and linear pharmacokinetics at high doses following single doses; (2) very large apparent volume of distribution at low doses, which decreases quickly as dose increases and reaches a limit at high

### A. Single Ascending Dose (SAD)



### B. Multiple Ascending Dose (MAD)

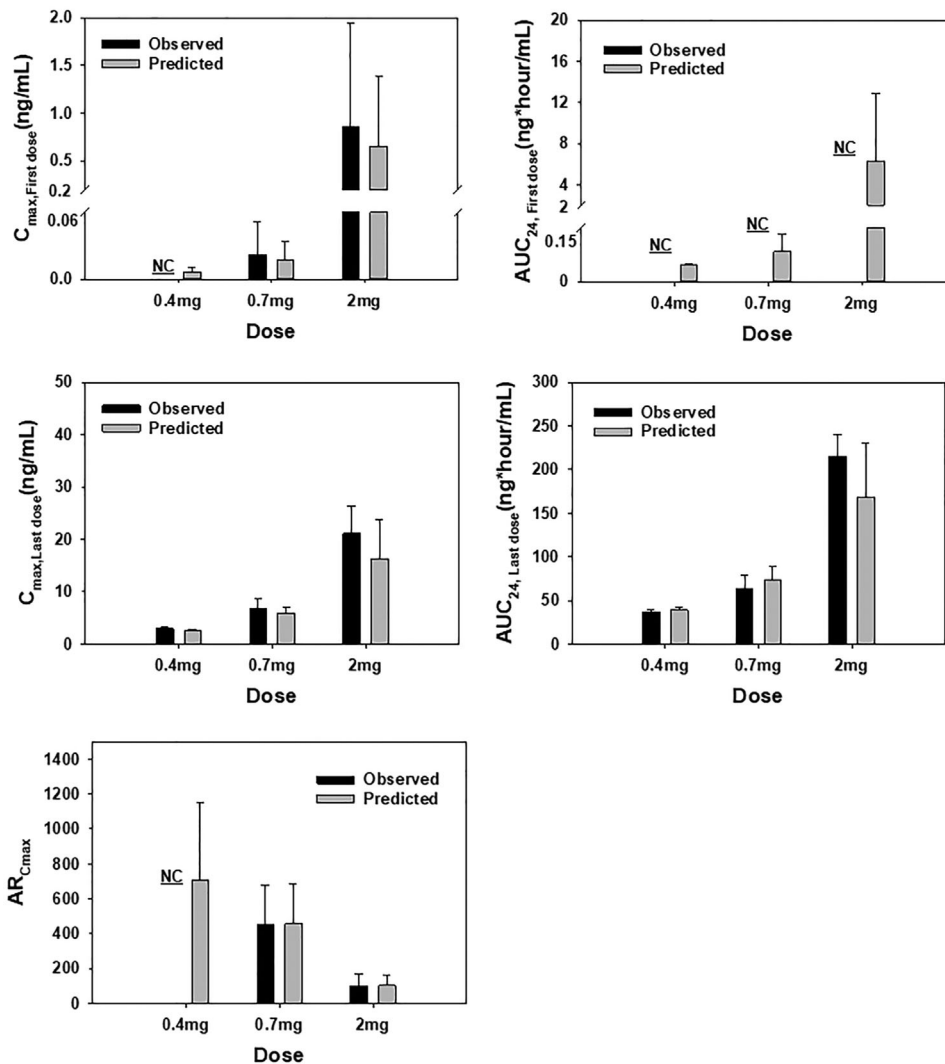


**Figure 7.** SPI-62 major pharmacokinetic parameters obtained by noncompartmental analysis of the observed concentration-time data (black) and predicted concentration-time data obtained from population pharmacokinetic model fitting (gray) using data from (A) the SAD trial and (B) the MAD trial. For each dose group, data are presented as mean and standard deviation ( $n = 4$  for 0.4-mg multiple dose group and  $n = 6$  for the other groups). NC, not calculated.

doses; (3) nonlinear PK following the first dose, but linear PK after repeated doses; and (4) unusually high accumulation of drug following repeated low doses, which cannot be explained by the compound's known half-life.<sup>14-16</sup> Using these general features as the "diagnostic tool," it is self-evident that the "symptoms" of the nonlinear pharmacokinetics observed in SPI-62 are fully in line with the TMDD principles for small-molecule compounds with targets located in tissues. The unusual PK of SPI-62 is not unique. Similar nonlinear PK behaviors have also been observed in other HSD-1 inhibitors, notably ABT-384<sup>17,18</sup> and MK-0916.<sup>19</sup> We have reported population PK modeling of ABT-384, and the structure of the final model for ABT-384 was also a 2-compartment TMDD model with 3 transit absorption compartments,<sup>18</sup> which is identical to what we established here for SPI-62. In addition to the HSD-1 inhibitors mentioned above, many small-molecule compounds from other classes have also been reported with nonlinear PK imparted by TMDD, such as warfarin, selegiline, imirestat, bosentan, linagliptin, and a series of soluble epoxide hydrolase inhibitors.<sup>16,20-25</sup>

We anticipate that the high-affinity, low-capacity site that leads to the nonlinear PK of SPI-62 is its pharmacological target, HSD-1. In general, the pharmacological TMDD of a compound cannot be concluded from the pharmacokinetic profiles alone. However, when strikingly similar unusual pharmacokinetics were observed in a group of structurally different compounds (ie, SPI-62, ABT-384, MK-0916), the evidence of HSD-1-mediated nonlinear PK, even though indirect, is compelling. In addition, the PD data of SPI-62 obtained from the SAD and MAD clinical studies also indicate that its nonlinear PK is likely mediated by its pharmacological target, HSD-1. For example, significant HSD-1 inhibition following a single dose of SPI-62 1 mg was observed even though plasma levels were below the level of quantification.<sup>12</sup> Persistent and almost complete inhibition on hepatic HSD-1 activity was observed, even at a daily dose of 0.2 mg of SPI-62.<sup>12</sup> These results indicated that substantial nonlinear pharmacokinetics of SPI-62 occurring at low doses reflect the extent of HSD-1 target occupancy.

Our model provided reasonable fitting for the single-dose data and most doses evaluated in the multiple-dose study, except the day 1 data from the 0.7-mg dose group. The inadequate fitting may have been caused by the higher percentage of below the limit of quantification (BLQ) data on day 1 in the lowest-dose groups. Several methods have been proposed in the literature for handling BLQ measures during model development.<sup>26,27</sup> We have explored those methods and

found that replacing the BLQ with LLOQ/2 provides the best model fitting. Based on our final TMDD model, the estimated target capacity ( $R_{tot}$ ), 6070 nmol, corresponds to approximately 2.5 mg of SPI-62, which comports well with the dose range in which pharmacokinetic nonlinearity is prominent. The estimated dissociation equilibrium constant ( $K_{off}/K_{on}$ ), 35.1 pM, is substantially lower than the measured  $K_i$  of 5.3 nM. Observed achievement of full and persistent liver HSD-1 inhibition following SPI-62 daily doses as low as 0.2 mg<sup>12</sup> indicates that SPI-62 remains tightly bound to and dissociates slowly from its target and suggests that the dissociation equilibrium constant is a more appropriate estimate of SPI-62 potency.

For small-molecule compounds undergoing pharmacological TMDD, PK information is important as their PK ties closely with PD and can provide valuable insight into target engagement. The nonlinear kinetics occurring at low doses is a strong sign of significant target engagement. SPI-62 SAD/FE and MAD studies also evaluated the PD effect of SPI-62. SPI-62 achieved almost complete inhibition of liver HSD-1, measured using the urinary ratio of cortisol (HSD-1 product) metabolites to cortisone (HSD-1 substrate) metabolites after multiple daily doses, even at the lowest tested dose of 0.2 mg SPI-62. Furthermore, substantial inhibition persisted throughout follow-up for up to 16 days after the last SPI-62 dose.<sup>12</sup> Single low doses of SPI-62 achieved complete and persistent occupancy of brain HSD-1, measured by competition with an HSD-1-specific PET ligand (data on file). Those observations are consistent with TMDD for SPI-62. They also indicate the importance of the TMDD model's strong predictive value for the PK of low SPI-62 doses. Our next step is to build a population PK/PD model of SPI-62 that will enable clinical dose selection by thorough evaluation of the quantitative relationship among dose, concentration, and HSD-1 tissue activity.

In summary, a TMDD model was successfully established to explain the substantial and unusual nonlinear PK of SPI-62 in healthy adults, and our modeling work has provided a strong foundation for dose selection in future SPI-62 clinical trials.

## Conflicts of Interest

David A. Katz is a Sparrow Pharmaceuticals employee, officer, and shareholder.

## Funding

This work was supported by a Sparrow Pharmaceuticals grant to the University of Iowa Pharmaceuticals Development Consortium (UIPDC).

## Authors' Contributions

- Conception and design of the work: Katz, An.
- Analysis of the data: Wu, An.
- Interpretation of the data: An, Katz, Wu.
- Drafting and critical revision of the manuscript: An, Katz.

## Data-Sharing Statement

The data will not be made available to other investigators.

## References

1. Tomlinson JW, Walker EA, Bujalska IJ, et al. 11beta-hydroxysteroid dehydrogenase type 1: a tissue-specific regulator of glucocorticoid response. *Endocr Rev.* 2004;25(5):831-866.
2. Basu R, Singh RJ, Basu A, et al. Splanchnic cortisol production occurs in humans: evidence for conversion of cortisone to cortisol via the 11-beta hydroxysteroid dehydrogenase (11beta-hsd) type 1 pathway. *Diabetes.* 2004;53(8):2051-2059.
3. Newell-Price J, Bertagna X, Grossman AB, Nieman LK. Cushing's syndrome. *Lancet.* 2006;367(9522):1605-1617.
4. Delivanis DA, Athimulam S, Bancos I. Modern management of mild autonomous cortisol secretion. *Clin Pharmacol Ther.* 2019;106(6):1209-1221.
5. Diederich S, Eigendorff E, Burkhardt P, et al. 11beta-hydroxysteroid dehydrogenase types 1 and 2: an important pharmacokinetic determinant for the activity of synthetic mineralocorticoids. *J Clin Endocrinol Metab.* 2002;87(12):5695-5701.
6. Weiss AJ, Elixhauser A, Bae J, Encinosa W. Origin of adverse drug events in U.S. hospitals, 2011. In: *Healthcare Cost and Utilization Project (HCUP) Statistical Briefs.* Rockville, MD: Agency for Healthcare Research and Quality; 2006 Feb; 2013.
7. Tomlinson JW, Draper N, Mackie J, et al. Absence of Cushingoid phenotype in a patient with Cushing's disease due to defective cortisone to cortisol conversion. *J Clin Endocrinol Metab.* 2002;87(1):57-62.
8. Arai H, Kobayashi N, Nakatsuru Y, et al. A case of cortisol producing adrenal adenoma without phenotype of Cushing's syndrome due to impaired 11beta-hydroxysteroid dehydrogenase 1 activity. *Endocr J.* 2008;55(4):709-715.
9. Song Z, Gong Y, Liu H, Ren Q, Sun X. Glycyrrhizin could reduce ocular hypertension induced by triamcinolone acetonide in rabbits. *Mol Vis.* 2011;17:2056-2064.
10. Tiganeşcu A, Hupe M, Uchida Y, Mauro T, Elias PM, Holleran WM. Topical 11beta-hydroxysteroid dehydrogenase type 1 inhibition corrects cutaneous features of systemic glucocorticoid excess in female mice. *Endocrinology.* 2018;159(1):547-556.
11. Morgan SA, McCabe EL, Gathercole LL, et al. 11beta-HSD1 is the major regulator of the tissue-specific effects of circulating glucocorticoid excess. *Proc Natl Acad Sci U S A.* 2014;111(24):E2482-2491.
12. Bellaire S, Walzer M, Wang T, Krauwinkel W, Yuan N, Marek GJ. Safety, pharmacokinetics, and pharmacodynamics of ASP3662, a Novel 11beta-hydroxysteroid dehydrogenase type 1 inhibitor, in healthy young and elderly subjects. *Clin Translat Sci.* 2019;12(3):291-301.
13. Levy G. Pharmacologic target-mediated drug disposition. *Clin Pharmacol Ther.* 1994;56(3):248-252.
14. An G. Concept of pharmacologic target-mediated drug disposition in large-molecule and small-molecule compounds. *J Clin Pharmacol.* 2020;60(2):149-163.
15. Bach T, Jiang Y, Zhang X, An G. General pharmacokinetic features of small-molecule compounds exhibiting target-mediated drug disposition (TMDD): A simulation-based study. *J Clin Pharmacol.* 2019;59(3):394-405.
16. An G. Small-molecule compounds exhibiting target-mediated drug disposition (TMDD): a minireview. *J Clin Pharmacol.* 2017;57(2):137-150.
17. An G, Liu W, Dutta S. Small-molecule compounds exhibiting target-mediated drug disposition - A case example of ABT-384. *J Clin Pharmacol.* 2015;55(10):1079-1085.
18. An G, Liu W, Katz DA, Marek GJ, Awni W, Dutta S. Population pharmacokinetics of the 11beta-hydroxysteroid dehydrogenase type 1 inhibitor ABT-384 in healthy volunteers following single and multiple dose regimens. *Biopharm Drug Dispos.* 2014;35(7):417-429.
19. Wright DH, Stone JA, Crumley TM, et al. Pharmacokinetic-pharmacodynamic studies of the 11beta-hydroxysteroid dehydrogenase type 1 inhibitor MK-0916 in healthy subjects. *Br J Clin Pharmacol.* 2013;76(6):917-931.
20. Levy G, Mager DE, Cheung WK, Jusko WJ. Comparative pharmacokinetics of coumarin anticoagulants I: Physiologic modeling of S-warfarin in rats and pharmacologic target-mediated warfarin disposition in man. *J Pharm Sci.* 2003;92(5):985-994.
21. Mager DE, Jusko WJ. General pharmacokinetic model for drugs exhibiting target-mediated drug disposition. *J Pharmacokinetic Pharmacodyn.* 2001;28(6):507-532.
22. Laine K, Anttila M, Huupponen R, Maki-Ikola O, Heinonen E. Multiple-dose pharmacokinetics of selegiline and desmethylselegiline suggest saturable tissue binding. *Clin Neuropharmacol.* 2000;23(1):22-27.
23. Weber C, Schmitt R, Birnboeck H, et al. Pharmacokinetics and pharmacodynamics of the endothelin-receptor antagonist bosentan in healthy human subjects. *Clin Pharmacol Ther.* 1996;60(2):124-137.
24. Wu N, Hammock BD, Lee KSS, An G. Simultaneous target-mediated drug disposition model for two small-molecule compounds competing for their pharmacological target: Soluble epoxide hydrolase. *J Pharmacol Exp Ther.* 2020;374(1):223-232.
25. Retlich S, Duval V, Graefe-Mody U, Jaehde U, Staab A. Impact of target-mediated drug disposition on Linagliptin pharmacokinetics and DPP-4 inhibition in type 2 diabetic patients. *J Clin Pharmacol.* 2010;50(8):873-885.
26. Ahn JE, Karlsson MO, Dunne A, Ludden TM. Likelihood based approaches to handling data below the quantification limit using NONMEM VI. *J Pharmacokinetic Pharmacodyn.* 2008;35(4):401-421.
27. Bergstrand M, Karlsson MO. Handling data below the limit of quantification in mixed effect models. *AAPS J.* 2009;11(2):371-380.

## Supplemental Information

Additional supplemental information can be found by clicking the Supplements link in the PDF toolbar or the Supplemental Information section at the end of web-based version of this article.